Prospective of ^{31}P MR Spectroscopy in Hepatopancreatobiliary Cancer: A Systematic Review of the Literature

Leonard W. F. Seelen, MD,[1,2] Lieke van den Wildenberg, MS,[1] Wybe J. M. van der Kemp, PhD,[1] Firdaus A. A. Mohamed Hoesein, MD, PhD,[2] Nadia Haj Mohammad, MD, PhD,[3] I. Quintus Molenaar, MD, PhD,[2] Hjalmar C. van Santvoort, MD, PhD,[2] Jeanine J. Prompers, PhD,[1*] and Dennis W. J. Klomp, PhD[1*]

Background: The incidence of liver and pancreatic cancer is rising. Patients benefit from current treatments, but there are limitations in the evaluation of (early) response to treatment. Tumor metabolic alterations can be measured noninvasively with phosphorus (^{31}P) magnetic resonance spectroscopy (MRS).
Purpose: To conduct a quantitative analysis of the available literature on ^{31}P MRS performed in hepatopancreatobiliary cancer and to provide insight into its current and potential for therapy (non-) response assessment.
Population: Patients with hepatopancreatobiliary cancer.
Field Strength/Sequence: ^{31}P MRS.
Assessment: The PubMed, EMBASE, and Cochrane library databases were systematically searched for studies published to 17 March 17, 2022. All ^{31}P MRS studies in hepatopancreatobiliary cancer reporting ^{31}P metabolite levels were included.
Statistical Tests: Relative differences in ^{31}P metabolite levels/ratios between patients before therapy and healthy controls, and the relative changes in ^{31}P metabolite levels/ratios in patients before and after therapy were determined.
Results: The search yielded 10 studies, comprising 301 subjects, of whom 132 (44%) healthy volunteers and 169 (56%) patients with liver cancer of various etiology. To date, ^{31}P MRS has not been applied in pancreatic cancer. In liver cancer, alterations in levels of ^{31}P metabolites involved in cell proliferation (phosphomonoesters [PMEs] and phosphodiesters [PDEs]) and energy metabolism (ATP and inorganic phosphate [Pi]) were observed. In particular, liver tumors were associated with elevations of PME/PDE and PME/Pi compared to healthy liver tissue, although there was a broad variety among studies (elevations of 2%–267% and 21%–233%, respectively). Changes in PME/PDE in liver tumors upon therapy were substantial, yet very heterogeneous and both decreases and increases were observed, whereas PME/Pi was consistently decreased after therapy in all studies (−13% to −76%).
Data Conclusion: ^{31}P MRS has great potential for treatment monitoring in oncology. Future studies are needed to correlate the changes in ^{31}P metabolite levels in hepatopancreatobiliary tumors with treatment response.
Evidence Level: 3
Technical Efficacy: Stage 2

J. MAGN. RESON. IMAGING 2023;57:1144–1155.

View this article online at wileyonlinelibrary.com. DOI: 10.1002/jmri.28372

Received Apr 20, 2022, Accepted for publication Jul 14, 2022.

*Address reprint requests to: D.W.J.K. & J.J.P, Department of Radiology, UMC Utrecht Cancer Center, The Netherlands. E-mails: d.w.j.klomp-2@umcutrecht.nl; j.j.prompers@umcutrecht.nl
Jeanine J. Prompers and Dennis W.J. Klomp contributed equally to this study.

From the [1]Department of Radiology, University Medical Center Utrecht, Utrecht, The Netherlands; [2]Department of Surgery, UMC Utrecht Cancer Center and St Antonius Hospital Nieuwegein: Regional Academic Cancer Center Utrecht, Utrecht, The Netherlands; and [3]Department of Medical Oncology, UMC Utrecht Cancer Center, Regional Academic Cancer Center Utrecht, Utrecht, The Netherlands

The incidence of hepatocellular carcinoma (HCC) and intrahepatic cholangiocarcinoma (ICC) is increasing in Western countries and even tripled in the United States since 1980.[1,2] For these types of cancer, treatment options such as surgical resection, transplantation, ablation, trans-arterial chemoembolization, and systemic therapy have proven to increase survival.[3–6] Worldwide, the (m)RECIST 1.1 criteria, which are based on computed tomography (CT) or magnetic resonance imaging (MRI) of (viable) tumor shrinkage or growth, are the most used criteria for cancer therapy response assessment.[7,8] However, these criteria have limitations due to delayed impact of treatment on tumor growth, resulting in misclassification of tumor response in patients.[9] Therefore, (m)RECIST 1.1 cannot timely predict oncological treatment effects.[10,11]

Next to primary tumors in the liver, the liver is one of the most common sites for metastatic disease and the most observed distant recurrence location after pancreatic cancer resection.[12–14] Currently, a shift in incidence rates among cancers is taking place and a trend of rising incidence and mortality from pancreatic cancer is seen.[15,16] For pancreatic cancer, the only curative treatment is complete surgical removal of the tumor. However, because of the surrounding vessels, the cancer is often not resectable. With FOLFIRINOX chemotherapy (fluorouracil, oxaliplatin, irinotecan, and leucovorin), tumor reduction can often be achieved, resulting in a resection rate up to 26% (95% CI: 20%–32%).[17] The first standard follow-up with CT following induction chemotherapy takes place after 2 months. At that point, patients may show progression on CT. A reliable early (i.e. before 2 months of therapy) response marker is not available.

A highly sensitive and timely evaluation of (early) tumor response assessment to systemic therapy and novel therapies for pancreatic and liver cancer is currently lacking. Several studies in various cancer types (bone, breast, liver, and brain tumors) have shown that tumor metabolic alterations caused by drug treatment can be detected by phosphorus (^{31}P) magnetic resonance spectroscopy (MRS).[18] Acquisition and analysis techniques for hepatic ^{31}P MRS have been reviewed before[19,20] and attempts have been made to standardize ^{31}P MRS protocols for cancer research.[21] ^{31}P MRS gives a unique, noninvasive view on tissue energy metabolism through the detection of phosphocreatine (PCr), adenosine triphosphate (ATP, with α-, β-, and γ-resonances) and inorganic phosphate (Pi). Moreover, it allows measurement of signals from cell membrane precursors, the phosphomonoesters (PMEs), and cell membrane degradation products, the phosphodiesters (PDEs). An increased PME/PDE ratio, indicative of cell proliferation, is a characteristic feature of tumor tissue and a reduction in PME/PDE during therapy has been demonstrated to be a marker of therapy response in breast cancer.[22–24] Importantly, changes in ^{31}P metabolites during treatment have been shown to take place well before morphological changes can be observed.[25–27] ^{31}P MRS could thus possibly be of help to assess effects of therapy for pancreatic and liver cancer in an early stage, thereby optimizing treatment efficacy and reducing unnecessary side effects of ineffective treatments.

The aim of this systematic review is to conduct a quantitative analysis of the available literature on ^{31}P MRS performed in hepatopancreatobiliary cancer and to provide insight into the current status of ^{31}P MRS and its potential for therapy (non-)response assessment.

Materials and Methods

Study Selection

A systematic search was performed in PubMed, Embase, and The Cochrane Library up to March 17, 2022. The study was conducted according to the Preferred Reporting Items for Systematic Reviews and Meta-Analyses (PRISMA) guidelines.[28]

The following search terms were used: (Phosphorus OR 31P OR phosphorus-31 OR Phosphorus Imaging OR 31P-MRS OR 31P-NMR) AND (Pancreas OR Pancreatic OR Liver OR Hepatic OR Biliary Tract) AND (Cancer OR Tumor OR Tumour). The search was restricted to title and abstract. After removing duplicates of the retrieved articles, one author (L.S.) assessed the relevance of the articles by the in- and exclusion criteria (Fig. 1). References of the studies included in this review were also cross-checked for inclusion. If multiple studies were published by the same author, exclusion of the overlapping data took place.

Eligibility Criteria

Studies were eligible when reporting on localized ^{31}P MRS in pancreatic and/or liver cancer. Second, ^{31}P metabolite levels (eg ATP, PME, PDE, etc.) or ratios (eg PME/ATP, PDE/ATP, PME/PDE, etc.) had to be evaluable. Animal studies, studies reporting data of in vitro experiments, and reviews were excluded. Articles written in non-English language were also excluded. Doubts about inclusion of studies were addressed by discussion and consensus in a regular meeting with the contributing authors.

Study Characteristics Extraction

The following study characteristics were extracted from the selected articles: first author, country, patient diagnosis, number of patients and healthy controls, age, sex, therapy, MRI field strength, ^{31}P radiofrequency (RF) coil, ^{31}P MRS method and parameters, and time point of performing ^{31}P MRS.

Data Extraction and Presentation

^{31}P metabolite levels and/or metabolic ratios were extracted from the selected articles. Methods for acquisition and quantification differed among the studies and not all details were always reported. To be able to directly compare the results from the different studies, we therefore report relative differences in reported ^{31}P metabolite levels/ratios between patients before therapy and healthy controls, and the relative changes in reported ^{31}P metabolite levels/ratios in patients before and after therapy, expressed as percentages. Metabolite ratios that were not reported were derived from the separate metabolite

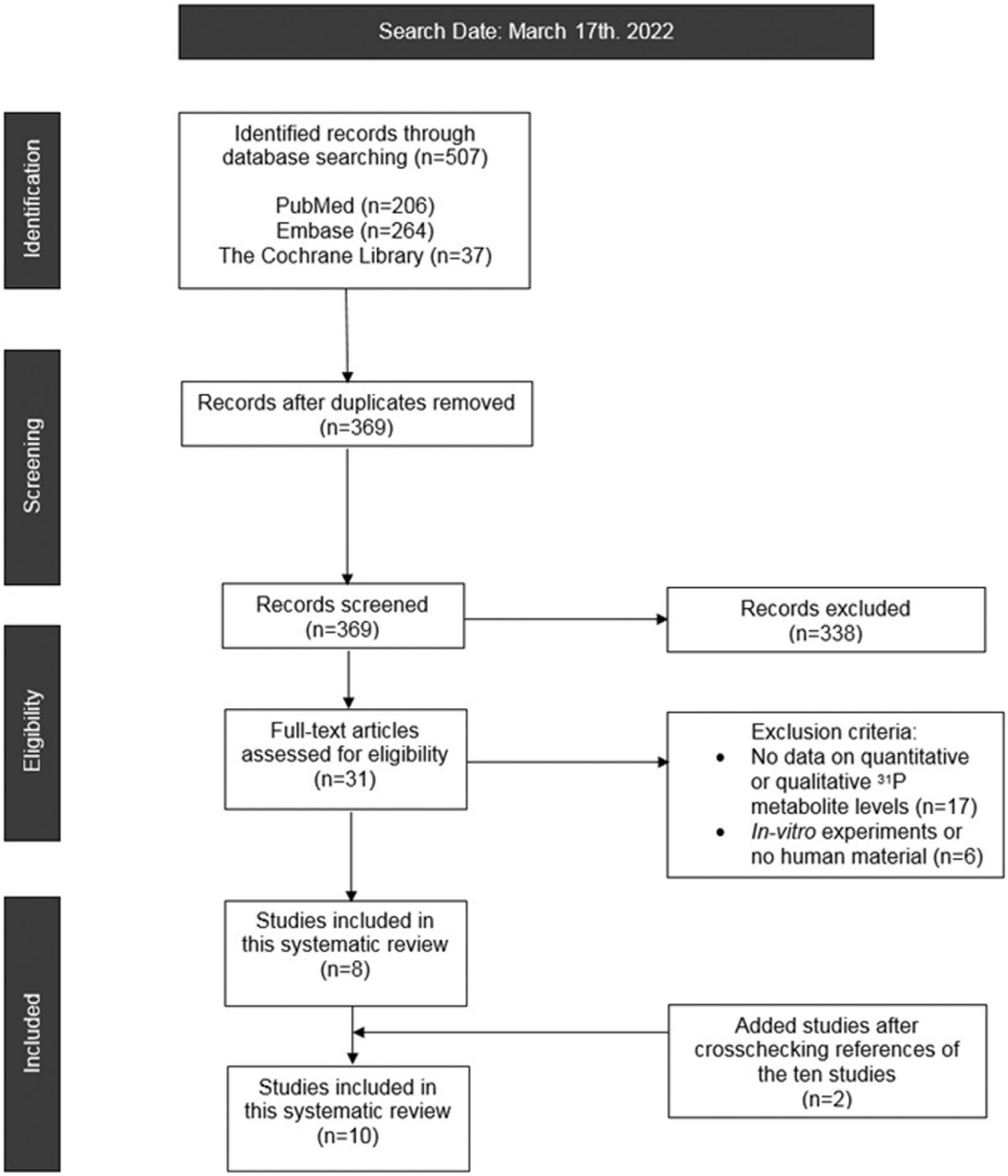

FIGURE 1: Flow diagram of study inclusion.

levels or from metabolite ratios with respect to ATP whenever those were available.

Results

Study Selection

The systematic search yielded a total of 507 studies: 206 articles from PubMed, 264 from Embase and 37 from The Cochrane Library. After exclusion of duplicates and screening of title and abstract, 31 full-text articles were assessed for eligibility. Of these studies, 23 (74%) were excluded due to no data on ^{31}P metabolite levels ($n = 17$) or lack of in vivo data ($n = 6$). At last, two studies[29,30] were added after been found eligible by crosschecking references of the 8 studies, resulting in 10 included studies.[29–38] The flow diagram of study inclusion in this systematic review is presented in Fig. 1.

Study Characteristics

No studies were found on the application of ^{31}P MRS in pancreatic tumors. The included studies (Table 1) were thus all on liver cancer and comprised 301 subjects, of whom 169 (56%) patients with liver cancer of various etiology and 132 (44%) healthy control subjects. Of the patients, 96 (57%) were diagnosed with liver metastases, 31 (19%) with HCC, 9 with adenocarcinoma (of unknown primary

TABLE 1. Study Characteristics

Author (year)	Country	Diagnosis	Subjects (*n*)	Patients (%)	Age (years) Mean (Range)	Male *n* (%)	MR Field Strength	^{31}P RF coil	Localization Method	Voxel Size	Flip Angle	TR (msec)	Time point of MRS (*n*)
Ljungberg (2012)	Sweden	Liver metastasis	11	11 (100%)	61 (29–73)	5 (45%)	1.5 T	Tx/Rx: 14 cm or 10 cm circular surface coil	ISIS	260–560 mL	90°	1500	Before, 1 and 3 days after HAE (11)
Yuan (2011)	China	HCC	15	15 (100%)[b]	53.2 (35–76)	13 (87%)	1.5 T	Tx/Rx: circular surface coil (size NS)	1D CSI	NS	NS	2000	Before and after chemoembolization (15)
Panda (2012)	USA	HCC	5	2 (40%)	46.8 (26–78)	2 (40%)	3 T	Tx: two 30 cm loop coils; Rx: 2 × 4 receive elements within the loop coils	2D CSI with slice selection	19 mL	NS	1000	Before therapy (1), other patient NS
Brinkmann (1995)	Germany	Liver metastasis	44	24 (55%)	45 (NR)	19 (43%)	1.5 T	Tx/Rx: 15 cm surface coil	Modified ISIS	146–158 mL	45°	600	Before therapy (24)
Meyerhoff (1992)	USA	Multiple tumors[a]	18	5 (28%)	NR (22–53)	NR	2 T	Tx/Rx: 14 cm surface coil	ISIS	NS	90°	1000	Before therapy (4) and after therapy (3)
Brinkmann (1992)	Germany	Various etiology[c]	46	28 (61%)	44.9 (NR)	17 (37%)	1.5 T	Tx/Rx: 15 cm surface coil	Modified ISIS (ILOPS)	158–196 mL	45°	600	Before therapy (28)
Schilling (1992)	Germany	Various etiology[d]	30	12 (40%)	54.5 (38–79)[e]	7 (58%)[e]	1.5 T	Tx/Rx: 12 cm surface coil	FROGS	Unlocalized	NS	3000	Before (12), up to 24 hours and 3 days after therapy (12)
Dixon (1991)	Australia	Hepatic lymphoma	47	22 (47%)	NR (16–81)	15 (68%)[e]	1.9 T	Tx: 15 cm surface coil; Rx: 6.5 cm surface coil	Rotating frame depth selection	NS	90°	1000	Before (any) treatment (22) and after treatment (11)
Francis (1991)	USA	Liver metastasis[f]	44	37 (84%)	50 (19–81)	NR	1.5 T	Tx/Rx: 8 cm or 14 cm surface coil	1D CSI	1 cm slices	NS	500	At time of initial discovery of the tumor (13) or recently undergone treatment (24)
Cox (1990)	United Kingdom	Various etiology[g]	70	42 (60%)	NR (18–72)	48 (69%)	1.6 T	Tx: saddle shaped coil; Rx: 6 cm or 15 cm surface coil	1D CSI or 3D CSI	2 or 3 cm slices 8 or 27 mL	45°	1000	Before (any) treatment (49) and after treatment (4)

NS = not specified; NR = not reported; HV = healthy volunteer; P = patient; HAE = hepatic arterial embolization.
[a]Include: Liver metastasis of colorectal cancer (2), hepatocellular carcinoma (2), adenocarcinoma of unknown primary (1).
[b]15 patients, 17 lesions.
[c]Include: Diffuse liver disease (cirrhosis, fatty liver) (5), focal liver disease: liver metastasis (19), unknown primary tumor (1), hemangioma, infarction, gallbladder empyema.
[d]Include: Hepatocellular carcinoma (2), liver metastasis (10).
[e]Characteristics from patient group alone.
[f]Include: Metastases form various primary tumors (eg colorectal cancer, neuroendocrine tumors) (30), hepatocellular carcinoma (7).
[g]Include: Focal lesions: (cholangiocarcinoma (2), hepatocellular carcinoma (3), adenocarcinoma (7), carcinoid (7), lymfhoma (2), endocrine adenomatosis (1), alcoholic (10), autoimmune (5), miscellaneous liver disorders (5)).

tumor) (5%), 24 (14%) with hepatic lymphoma, 7 (4%) with a carcinoid, and 2 (1%) with a cholangiocarcinoma. Not all studies published the mean age of the subjects.[29,30,35] Of those who did, the mean age varied from 50 years to 61 years, with the biggest age range seen in the study of Dixon et al[29] (16–81 years). Magnetic field strengths of 1.5–3 T were used. Most studies made use of ^{31}P RF transmit and receive surface coils, with diameters ranging between 6 and 30 cm. Volume localization for ^{31}P MRS was achieved using slice selection or suppression, single-voxel localization (i.e. image-selected in vivo spectroscopy [ISIS] or modified ISIS) or 1D, 2D, or 3D chemical shift imaging (CSI) approaches. For the studies with 3D spatial localization, the nominal voxel sizes ranged between 8 and 560 mL. Flip angles and repetition times varied among studies. In the patients, ^{31}P MRS was performed before therapy, or both before and after therapy, except for the study of Francis et al.[38] In the latter study, only data were reported during/after therapy, which could therefore not be used to calculate relative differences (between patients before therapy and healthy controls) or changes (before and after therapy). Treatment consisted of chemotherapy, chemoembolization or hepatic arterial embolization (dependent on the cancer type). All studies reported if a patient underwent ^{31}P MRS at initial discovery of the tumor or during treatment. A specific diet was followed in five studies.[30–32,36,37]

^{31}P Metabolite Levels in Liver Cancer

Methods for metabolite quantification differed among the studies, for example, peak areas were determined by either integration or fitting, and metabolite levels were expressed as metabolite ratios or individual metabolite levels in some cases. In the studies reporting individual metabolite levels, either the total phosphate signal was used for normalization[33,37] or absolute quantification was performed based on the calculated coil sensitivity.[35] To be able to directly compare the results from the different studies, we therefore calculated relative differences/changes in the reported ^{31}P metabolite levels/ratios.

Table 2 shows relative differences in ^{31}P metabolite levels or metabolic ratios in patients before therapy and healthy volunteers in the same study. For each metabolite or metabolic ratio, there was data available from at least two studies out of the seven eligible studies. The largest differences between patients and controls were observed in the PME/ATP, PME/Pi and PME/PDE ratios, but there was also large variability between the different studies: PME/ATP was 34%–200% higher, PME/Pi was 21%–233% higher (Fig. 2a), and PME/PDE was 2%–267% (Fig. 2b) higher in patients compared with controls. PDE/ATP and Pi/ATP ratios were either higher or lower in patients compared with controls and differences in these ratios were thus not consistent among the different studies. Only two studies report individual metabolite levels.[35,37] Schilling et al measured similar ATP levels and increased PME levels in patients compared to controls.[38] In contrast, the study of Meyerhoff et al[35] did not report a difference in PME levels between patients and controls but rather showed a lower ATP level in patients.

Table 3 shows relative changes in ^{31}P metabolite levels or metabolic ratios in patients before and after therapy in the same study. Six studies were eligible for assessing the treatment response and less patients were included than for the comparison between patients (before therapy) and healthy volunteers.[29,30,32,33,35,37] The timing of the ^{31}P MRS after therapy differed among the studies. In the study of Meyerhoff et al,[35] ATP, PME, and PDE levels dropped after therapy, whereas Pi remained stable. In contrast, in the study of Schilling et al[37] and Yuan et al,[33] Pi was increased after therapy. The Pi/ATP ratio increased after therapy in three studies (24%–88%),[30,35,37] and was unchanged in a fourth study.[33] PME/Pi ratios were decreased after therapy (−13% to −76%) in all studies where this ratio was available or could be derived (five out of the six studies) (Fig. 2a). PME/ATP and PDE/ATP ratios did not show consistent changes upon therapy. Likewise, the PME/PDE ratio decreased after therapy in two studies[29,35] but increased in two other studies,[33,37] and did not significantly change in another (Fig. 2b).[32]

Discussion

The current review provides an overview of quantitative ^{31}P MRS data in liver cancer. In liver cancer, substantial alterations in levels of ^{31}P metabolites involved in cell proliferation and energy metabolism have been observed. In particular, liver tumors were associated with an elevation of PME/PDE and PME/Pi compared to healthy liver tissue, although there was a broad variety among studies. Substantial changes in PME/PDE in liver tumors upon therapy were observed, showing both decreases and increases for the heterogonous treatments and measurement intervals among the included studies, whereas PME/Pi was decreased after therapy in all studies. To date, ^{31}P MRS has not been applied in pancreatic cancer.

As to our knowledge, Griffiths et al[39] published the first ^{31}P MRS study of tumors in a living rat in 1981. Two years later, they described the first application of in vivo ^{31}P MRS of a sarcoma in a hand.[40] It was the beginning of upcoming in vitro and in vivo ^{31}P MRS studies in several tumor types. Smith et al[41] compared in vivo and in vitro ^{31}P NMR spectra from human breast tumors and found that the contribution of PDEs was much lower in the in vitro spectra as compared with in vivo spectra. This was related to the fact that the in vivo PDE signal can contain contributions from mobile (high curvature) membrane phospholipids, which are not represented in aqueous extracts. Furthermore, it is difficult to

TABLE 2. Differences in Liver (Tumor) ^{31}P Metabolite Levels or Ratios Between Patients Before Therapy and Healthy Volunteers

Author (year)	Diagnosis	Patients	Age (years) mean (range)	Healthy Volunteers	Age (years) mean (range)	ATP	Pi	PME	PDE	Pi/ATP	PME/ATP	PDE/ATP	PME/Pi	PME/PDE
Panda[a] (2012)	HCC	1	78	3	33 (26–39)									↑↑ 61%
Brinkmann[b] (1995)	Liver metastasis[h]	24	55 (NR)	20	33 (NR)					↑ 10%	↑↑ 84%	↑ 34%	↑↑ **66%**	↑ **37%**
Meyerhoff[c] (1992)	Multiple tumors[i]	4	55.7 (51–63)	13	NR (22–55)	↓↓ −54%	↓ −26%	↑ 3%	↑ 1%	↑↑ **60%**	↑↑ 200%[m]	↑↑ **118%**	↑ 31%	↑ **2%**
Brinkmann[d] (1992)	Various etiology[j]	19	55.7 (NR)	18	29.3 (NR)					↑ 27%	↑↑ 53%	↑ 35%	↑ **21%**	↑ 28%
Schilling[e] (1992)	Liver metastasis[k]	12	54.5 (38–79)	18	NR	↓ −1%	↓ −7%	↑ 33%	↓ −3%	↓ **−6%**	↑ **34%**	↓ **−2%**	↑ **43%**	↑ **36%**
Dixon[f] (1991)	Hepatic lymphoma	22	42.9 (16–81)	25	NR (20–50)					↑ 6%	↑↑ 73%	↓ −6%	↑↑ 64%	↑↑ **85%**
Cox[g] (1990)	Various etiology[l]	20	NR*	28	NR (22–59)					↓ −19%	↑↑ 170%	↓ −27%	↑↑ **233%**	↑↑ 267%

NR = Not reported; NR* = Not reported in all patients; Bold = calculated from reported metabolite levels or metabolite-to-ATP ratios.
↓: decrease of <50%; ↓↓: decrease of ≥50%; ↑: increase of <50%; ↑↑: increase of ≥50%.
[a]Peak ratios (Gaussian fitting).
[b]Peak ratios (areas under the curve), β-ATP measured.
[c]Peak ratios and absolute concentrations (mmol/kg wet weight) (Gaussian fitting) γ-ATP measured.
[d]Peak ratios (areas under the curve), β-ATP measured.
[e]Relative peak areas as percentage (fitting).
[f]Peak ratios (triangulation), γ-ATP measured.
[g]Peak ratios (integration), β-ATP measured.
[h]Include: primary origin not specified (24).
[i]Include: Liver metastasis of colorectal cancer (1), hepatocellular carcinoma (2), adenocarcinoma of unknown primary (1).
[j]Include: liver metastasis of various etiology (19).
[k]Include: liver metastasis of colorectal cancer (12).
[l]Include: Focal lesions: cholangiocarcinoma (2), hepatocellular carcinoma (2), adenocarcinoma (7), carcinoid (7), lymfhoma (2).
[m]In three patients.

maintain integrity of cellular metabolites in vitro.[42] Consequently, despite the much lower sensitivity of ^{31}P MRS in vivo compared to in vitro, translation of in vitro observations to in vivo metabolism is questionable.

In all of the reviewed papers, the PME/PDE and PME/Pi ratios in patients with liver cancer (before therapy) was higher compared with the liver PME/PDE and PME/Pi ratios in healthy volunteers, although there was great variability with differences ranging from 2% to 267% (Fig. 2b) and 21%–233% (Fig. 2a), respectively. Upon therapy, a very heterogeneous response was observed in changes in PME/PDE ratios, including decreases, as may be expected, but also increases (Fig. 2b), whereas the PME/Pi ratios were consistently decreased after therapy (−13% to −76%) in all studies (Fig. 2a). The heterogeneous results may be related to the different etiologies of liver cancer included in the studies, that is, primary liver tumors and liver metastases, and the different types of therapy that have been applied, that is, chemo(radio) therapy, (chemo)embolization and hepatic arterial embolization (HAE). Also, the time point of scanning after therapy differed between and within the included studies. The optimal time point to perform ^{31}P MRS after the start of therapy remains to be established.

Only in two of the reviewed studies, the ^{31}P MRS results were related to treatment response. Ljungberg et al showed that before HAE, the PME/Pi ratio was significantly lower in responders than in nonresponders, which may reflect intrinsic differences in responsive and nonresponsive tumors.[33] However, 1 and 3 days after the start of HAE, PME/Pi ratios were no longer significantly different between

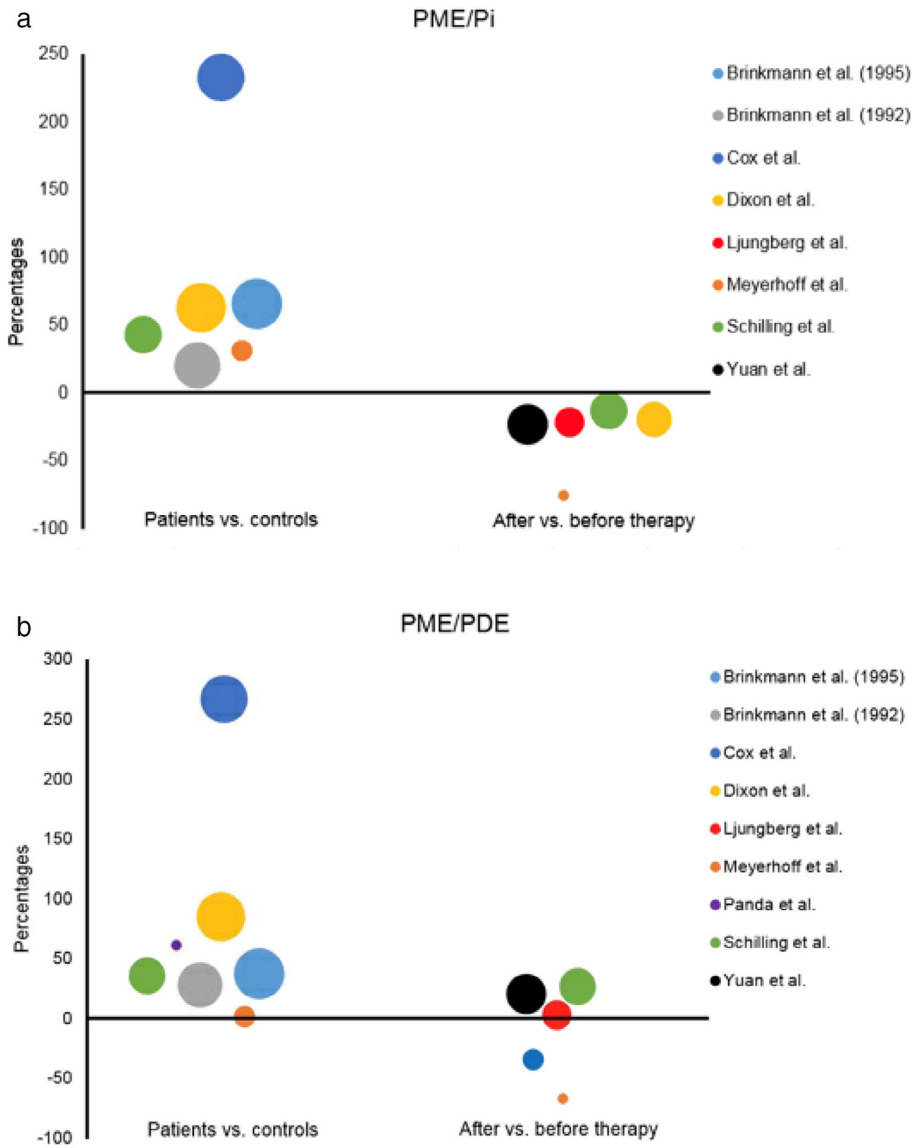

FIGURE 2: (a) Differences in PME/Pi between patients and controls and changes in PME/Pi for patients before and after therapy, and (b) differences in PME/PDE between patients and controls and changes in PME/PDE for patients before and after therapy, as derived from the reviewed literature. The surface of each sphere is scaled to the number of patients in the respective study.

TABLE 3. Changes in Liver Tumor ^{31}P Metabolite Levels or Ratios for Patients Before and After Therapy

Author (year)	Diagnosis	Patients	Age (years) mean (range)	Male (*n*), (%)	Patients (*n*) Treatment	ATP	Pi	PME	PDE	Pi/ ATP	PME/ ATP	PDE/ ATP	PME/Pi	PME/PDE
Ljungberg[a] (2012)	Liver metastasis[g]	8	62.3	4 (50%)	Hepatic arterial embolization (8)						↑ 17%		↓ −22%	↑ 3%
Yuan[b] (2011)	HCC	15[j]	53.2 (35–76)	13 (87%)	Chemoembolization (15[j])	↑ 21%	↑ 21%	↓ −6%	↓↓ −28%	= **0%**	↓ −19%[k]	↓↓ −33%[k]	↓ **−23%**	↑ **20%**[l]
Meyerhoff[c] (1992)	HCC	1	63	0	Chemoembolization (1)	↓↓ −46%	↑ 2%	↓↓ −76%	↓↓ −27%	↑↑ **88%**	↓↓ −47%	↑↑ **35%**	↓↓ **−76%**	↓↓ **-67%**[l]
Schilling[d] (1992)	Various etiology[h]	12	54.5 (38–79)	7 (58%)	5-FU (6), chemoembolization (6)	= 0%	↑↑25%	↑ 8%	↓ −15%	↑↑ **25%**	↑ **9%**	↓ **−15%**	↓ **−13%**	↑↑ **27%**[l]
Dixon[e] (1991)	Hepatic lymphoma	11	NR	NR	Chemotherapy NS (11)								↓ −19%	
Cox[f] (1990)	Various etiology[i]	4	NR	NR	5-FU (1), embolization (2), chemoradiotherapy (1)					↑ 24%				↓↓ −34%

NS = not specified; NR = not reported; FU = fluorouracil.
Bold = calculated from reported metabolite levels or metabolite-to-ATP ratios.
↓: decrease of <25%; ↓↓: decrease of ≥25%; ↑: increase of <25%; ↑↑: increase of ≥25%; =: no increase/decrease.
[a]Peak ratios (Lorentzian fitting).
[b]Peak ratios as percentage (Gaussian fitting) nucleoside triphosphates (NTP) measured.
[c]Peak ratios and absolute concentrations (mmol/kg wet weight) (Gaussian fitting) γ-ATP measured.
[d]Relative peak areas as percentage (fitting).
[e]Peak ratios (triangulation), γ-ATP measured.
[f]Peak ratios (integration), β-ATP measured.
[g]Include: liver metastasis of gastrinoma (1), midgut carcinoid (6), pancreatic tumor (1).
[h]Include: HCC (2) and metastases of unknown origin (10).
[i]Include: Focal lesions: adenocarcinoma (1), carcinoid (2), lymfhoma (1).
[j]17 lesions.
[k]Percentages of median values.
[l]Metabolites calculated after more than 3 days after therapy.

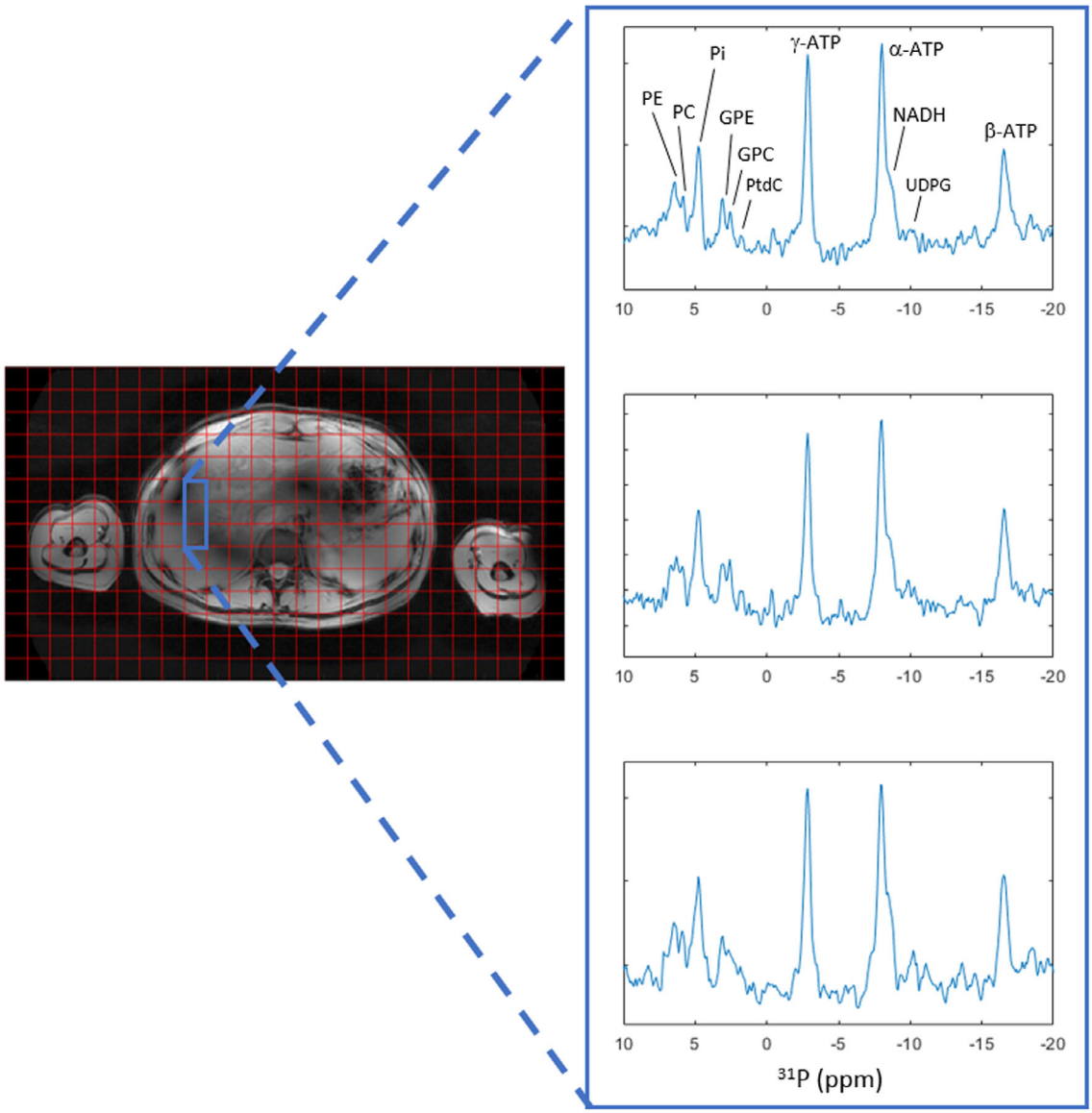

FIGURE 3: 3D ^{31}P CSI data of the liver from a healthy volunteer acquired at 7 T with a ^{31}P whole-body transmit coil in combination with a 16-channel ^{31}P receive array. The image shows one slice of a transversal T_1-weighted MRI scan overlaid with the ^{31}P CSI grid (nominal voxel size = 20 mm isotropic). ^{31}P MR spectra of three representative voxels in the liver (indicated by the blue rectangle) are shown on the right. Peak annotations: phosphoethanolamine (PE), phosphocholine (PC), inorganic phosphate (Pi), glycerophosphoethanolamine (GPE), glycerophosphocholine (GPC), phosphatidylcholine (PtdC), α-, β-, and γ-adenosine triphosphate (ATP), nicotinamide adenine dinucleotide (NADH), and uridine diphosphate glucose (UDPG). *Source*: Adapted from reference 51.

responders and nonresponders.[32] Yuan et al found no significant changes in ^{31}P metabolite levels/ratios after treatment in the nonresponsive group, whereas in the responders various ^{31}P metabolite levels/ratios were significantly changed upon therapy.[33] In the other studies, there was no information on treatment outcomes and therefore it is not clear whether the variability in the data upon treatment could in fact reflect differences in treatment response. In breast cancer, a negative preoperative indication for systemic therapy was highly accurate (96%) for tumors ≤2.0 cm with PME ≤ PDE as determined by ^{31}P MRS.[22] Moreover, in breast cancer patients, a decrease in PME/PDE was observed after 3 weeks of neoadjuvant chemotherapy for (partial) responders, whereas no significant change was detected for nonresponders.[24] For liver and pancreatic cancer, future studies should give insight into the relation between ^{31}P metabolite levels and treatment response.

Besides the differences in tumor etiologies and therapies, time point of scanning after therapy, and potential differences in therapy response, also the experimental setups and field strengths, ^{31}P MRS methods and parameters, and analyses methods differed greatly between studies. Volume localization for ^{31}P MRS was achieved using various methods (slice selection or suppression, single-voxel localization with ISIS, or 1D, 2D or 3D CSI) and for many studies voxel sizes were rather large, ranging up to 560 mL. Therefore, there can be

substantial partial volume effects, that is, signal from healthy tissue in the tumor voxel of interest, which can have reduced potential effect sizes, especially in focal lesions, and thus can have contributed to the observed variability. Even so, the method of using metabolite ratios is very robust, because it is less dependent on experimental variations, such as spatial sensitivity. Moreover, in comparison to widely available ^{1}H CSI, ^{31}P MRS is not hindered by the orders of magnitude larger signals of water and lipids that would obscure the metabolite detection, particularly in the presence of typical body motion and magnetic field inhomogeneities.[43] In none of the reported studies NOE enhancement or broadband proton decoupling was used. Although NOE enhancement can improve SNR, it may also influence metabolic ratios, which needs to be corrected for. Proton decoupling can substantially improve the spectral resolution, in particular in the PME and PDE regions at lower field strengths.[44] The reported studies were conducted at 1.5–3 T and because proton decoupling was not used, quantified PDE concentrations may have been affected by varying levels of phosphatidylcholine (also resonating in the PDE region), depending on the nutritional status of the subjects. It is currently not clear whether nutritional status plays an important role in ^{31}P MRS of liver or liver tumors. Brinkmann et al compared 3–5 hours fasting vs. overnight fasting, for which they did not find significant changes in the ratios of ^{31}P metabolites in healthy liver tissue or liver metastases.[45] Future studies are needed to determine whether nutritional status could influence ^{31}P metabolite levels.

While the motivation for in vivo detection of tumor metabolism is strong, and feasibility of in vivo detection of ^{31}P metabolites in tumors was already demonstrated decades ago, a relatively low number of papers could be found on ^{31}P MRS in liver cancer and no published ^{31}P MRS studies were found on localized pancreatic cancer. This may be due to several reasons: Sensitivity of ^{31}P MRS is low, so it requires either very large voxels and thus large tumors or increased sensitivity provided by ultra-high field MRI systems (eg 7 T). The first may limit patient inclusion and lack of clinical relevance. The second complicates setting up a clinical study, as ultra-high field MRI scanners have not yet obtained FDA or CE clearance for clinical use in the human body. However, most vendors have obtained FDA and CE clearance for using the 7 T MRI for brain applications, so xit may be straightforward to obtain these clearances for body applications as well. A critical review as reported here may help to justify these clearances. Recently, the first 7 T application of ^{31}P CSI in a liver metastasis was demonstrated in a case study, showing improved spectral resolution compared to lower field strengths, allowing separate detection of the individual PMEs (i.e. PC and PE) and PDEs (i.e. GPC and GPE)[46] An additional complication of ^{31}P MRS in the body is that the penetration depth of commonly used ^{31}P surface coils is limited, which makes ^{31}P MRS of deeper lying organs, such as the pancreas, challenging.[47,48] We have overcome this challenge by using an embedded ^{31}P whole-body transmit coil, producing a homogeneous radio-frequency field throughout the human body,[49] in combination with a 16-channel ^{31}P receive array[50] to acquire high spatial- and spectral resolution ^{31}P CSI data of the whole human liver at 7 T (Fig. 3).[51] Future development of motion correction techniques is expected to improve spectral quality in the presence of (respiratory) motion, such as for pancreatic tumors, and to reduce signal ghosting from tissues outside the regions of interest.

In conclusion, ^{31}P MRS has great potential in oncology for predicting or monitoring early tumor response of therapy (eg chemotherapy or immunotherapy). This review summarizes metabolic alterations as observed with ^{31}P MRS in liver metastases or liver tumors in patients either with respect to healthy controls or after therapy, obtained from 10 independent studies with a total of 301 included subjects. The next step is to find correlations of early metabolic alterations, as observed with ^{31}P MRS, with eventual treatment response, to establish if ^{31}P MRS is suitable for future clinical use in hepatopancreatobiliary cancer.

Acknowledgments

The authors thank the European Union, Dutch cancer society and Technical Sciences, and the St. Antonius Hospital Nieuwegein for financial support.

REFERENCES

1. Dasgupta P, Henshaw C, Youlden DR, Clark PJ, Aitken JF, Baade PD. Global trends in incidence rates of primary adult liver cancers: A systematic review and meta-analysis. Front Oncol 2020;10:171.
2. American Cancer Society. No Title [Internet]. Available from: https://www.cancer.org/cancer/liver-cancer/about/what-is-key-statistics.html
3. Solomon B, Soulen MC, Baum RA, Haskal ZJ, Shlansky Goldberg RD, Cope C. Chemoembolization of hepatocellular carcinoma with cisplatin, doxorubicin, mitomycin-C, ethiodol, and polyvinyl alcohol: Prospective evaluation of response and survival in a U.S. population. J Vasc Interv Radiol 1999;10(6):793-798.
4. Llovet JM, Bruix J. Systematic review of randomized trials for unresectable hepatocellular carcinoma: Chemoembolization improves survival. Hepatology 2003;37(2):429-442.
5. Llovet JM, Real MI, Montana X, et al. Arterial embolisation or chemoembolisation versus symptomatic treatment in patients with unresectable hepatocellular carcinoma: A randomised controlled trial. Lancet 2002;359:1734-1739.
6. Schwarz C, Fitschek F, Primavesi F, et al. Metachronous hepatic resection for liver only pancreatic metastases. Surg Oncol 2020;35:169-173.
7. Eisenhauer EA, Therasse P, Bogaerts J, et al. New response evaluation criteria in solid tumours: Revised RECIST guideline (version 1.1). Eur J Cancer 2009;45(2):228-247.
8. Lencioni R, Llovet JM. Modified RECIST (mRECIST) assessment for hepatocellular carcinoma. Semin Liver Dis 2010 Feb;30(1):52-60.

9. Rich NE, Parikh ND, Singal AG. Overdiagnosis: An understudied issue in hepatocellular carcinoma surveillance. Semin Liver Dis 2017;37(4): 296-304.
10. Gregory J, Dioguardi Burgio M, Corrias G, Vilgrain V, Ronot M. Evaluation of liver tumour response by imaging. JHEP Rep 2020;2(3):100100.
11. Ko CC, Yeh LR, Kuo YT, Chen JH. Imaging biomarkers for evaluating tumor response: RECIST and beyond. Biomark Res 2021;9(1):52.
12. Riihimäki M, Thomsen H, Sundquist K, Sundquist J, Hemminki K. Clinical landscape of cancer metastases. Cancer Med 2018;7(11):5534-5542.
13. Tanaka M, Mihaljevic AL, Probst P, et al. Meta-analysis of recurrence pattern after resection for pancreatic cancer. Br J Surg 2019;106(12): 1590-1601.
14. Groot VP, Rezaee N, Wu W, et al. Patterns, timing, and predictors of recurrence following pancreatectomy for pancreatic ductal adenocarcinoma. Ann Surg 2018;267(5):936-945.
15. Mizrahi JD, Surana R, Valle JW, Shroff RT. Pancreatic cancer. Lancet 2020;395(10242):2008-2020.
16. Rahib L, Wehner MR, Matrisian LM, Nead KT. Estimated projection of US cancer incidence and death to 2040. JAMA Netw Open 2021;4(4): e214708.
17. Chen Z, Lv Y, Li H, Diao R, Zhou J, Yu T. Meta-analysis of FOLFIRINOX-based neoadjuvant therapy for locally advanced pancreatic cancer. Medicine (Baltimore) 2021;100(3):e24068.
18. Negendank W. Studies of human tumors by MRS: A review. NMR Biomed 1992;5(5):303-324.
19. Solga SF, Horska A, Clark JM, Diehl AM. Hepatic 31P magnetic resonance spectroscopy: A hepatologist's user guide. Liver Int 2005;25(3): 490-500.
20. Valkovič L, Chmelík M, Kršňák M. In-vivo^{31}P-MRS of skeletal muscle and liver: A way for non-invasive assessment of their metabolism. Anal Biochem 2017;15(529):193-215.
21. Arias-Mendoza F, Zakian K, Schwartz A, et al. Methodological standardization for a multi-institutional in vivo trial of localized 31P MR spectroscopy in human cancer research. In vitro and normal volunteer studies. NMR Biomed 2004;17(6):382-391.
22. Schmitz AMT, Veldhuis WB, Menke-Pluijmers MBE, et al. Preoperative indication for systemic therapy extended to patients with early-stage breast cancer using multiparametric 7-tesla breast MRI. PLoS One 2017;12(9):e0183855.
23. van der Kemp WJ, Stehouwer BL, Luijten PR, et al. Detection of alterations in membrane metabolism during neoadjuvant chemotherapy in patients with breast cancer using phosphorus magnetic resonance spectroscopy at 7 tesla. Springerplus 2014;27(3):634.
24. Krikken E, van der Kemp WJM, van Diest PJ, et al. Early detection of changes in phospholipid metabolism during neoadjuvant chemotherapy in breast cancer patients using phosphorus magnetic resonance spectroscopy at 7T. NMR Biomed 2019;32:e4086.
25. Daly PF, Cohen JS. Magnetic resonance spectroscopy of tumors and potential *in vivo* clinical applications: A review. Cancer Res 1989;49: 770-779.
26. Semmler W, Gademann G, Bachert-Baumann P, Zabel HJ, Lorenz WJ, van Kaick G. Monitoring human tumor response to therapy by means of P-31 MR spectroscopy. Radiology 1988;166:533-539.
27. Steen RG. Response of solid tumors to chemotherapy monitored by in vivo ^{31}P nuclear magnetic resonance spectroscopy: A review. Cancer Res 1989;49:4075-4085.
28. Moher D, Shamseer L, Clarke M, et al. Preferred reporting items for systematic review and meta-analysis protocols (PRISMA-P) 2015 statement. Syst Rev 2015;4:1.
29. Dixon RM, Angus PW, Rajagopalan B, Radda GK. Abnormal phosphomonoester signals in 31P MR spectra from patients with hepatic lymphoma. A possible marker of liver infiltration and response to chemotherapy. Br J Cancer 1991;63(6):953-958.
30. Cox IJ, Menon DK, Sargentoni J, et al. Phosphorus-31 magnetic resonance spectroscopy of the human liver using chemical shift imaging techniques. J Hepatol 1992 Mar;14(2–3):265-275.
31. Brinkmann G, Melchert UH, Emde L, et al. In vivo P-31-MR-spectroscopy of focal hepatic lesions. Effectiveness of tumor detection in clinical practice and experimental studies of surface coil characteristics and localization technique. Invest Radiol 1995;30(1): 56-63.
32. Ljungberg M, Westberg G, Vikhoff-Baaz B, et al. 31P MR spectroscopy to evaluate the efficacy of hepatic artery embolization in the treatment of neuroendocrine liver metastases. Acta Radiol 2012;53(10):1118-1126.
33. Yuan Z, Ye XD, Dong S, Xu LC, Xiao XS. Evaluation of early imaging response after chemoembolization of hepatocellular carcinoma by phosphorus-31 magnetic resonance spectroscopy-initial experience. J Vasc Interv Radiol 2011;22(8):1166-1173.
34. Panda A, Jones S, Stark H, et al. Phosphorus liver MRSI at 3 T using a novel dual-tuned eight-channel ^{31}P/^{1}H H coil. Magn Reson Med 2012; 68(5):1346-1356.
35. Meyerhoff DJ, Karczmar GS, Valone F, et al. Hepatic cancers and their response to chemoembolization therapy. Quantitative image-guided 31P magnetic resonance spectroscopy. Invest Radiol 1992;27(6): 456-464.
36. Brinkmann G, Melchert UH. A study of T1-weighted 31phosphorus MR-spectroscopy from patients with focal and diffuse liver disease. Magn Reson Imaging 1992;10(6):949-956.
37. Schilling A, Gewiese B, Berger G, et al. Liver tumors: Follow-up with P-31 MR spectroscopy after local chemotherapy and chemoembolization. Radiology 1992;182(3):887-890.
38. Francis IR, Chenevert TL, Gubin B, et al. Malignant hepatic tumors: P-31 MR spectroscopy with one-dimensional chemical shift imaging. Radiology 1991;180(2):341-344.
39. Griffiths JR, Stevens AN, Iles RA, Gordon RE, Shaw D. 31P-NMR investigation of solid tumours in the living rat. Biosci Rep 1981;1(4): 319-325.
40. Griffiths JR, Cady E, Edwards RH, McCready V, Wilkie DR, Wiltshaw E. 31P-NMR studies of a human tumour in situ. Lancet 1983;1(8339): 1435-1436.
41. Smith TA, Glaholm J, Leach MO, et al. A comparison of in vivo and in vitro 31P NMR spectra from human breast tumours: Variations in phospholipid metabolism. Br J Cancer 1991;63(4):514-516.
42. Bell JD, Bhakoo KK. Metabolic changes underlying ^{31}P MR spectral alterations in human hepatic tumours. NMR Biomed 1998;11(7): 354-359.
43. Forner R, Nam K, de Koning KJ, et al. RF coil setup for ^{31}P MRSI in tongue cancer *in vivo* at 7 T. Front Neurol 2021;2(12):695202.
44. Li CW, Negendank WG, Murphy-Boesch J, Padavic-Shaller K, Brown TR. Molar quantitation of hepatic metabolites in vivo in proton-decoupled, nuclear Overhauser effect enhanced 31P NMR spectra localized by three-dimensional chemical shift imaging. NMR Biomed 1996;9(4):141-155.
45. Brinkmann G, Melchert UH, Muhle C, et al. Influence of different fasting periods on P-31-MR-spectroscopy of the liver in normals and patients with liver metastases. Eur Radiol 1996;6(1):62-65.
46. Rivera D, Kalleveen I, de Castro CA, et al. Inherently decoupled ^{1} H antennas and ^{31} P loops for metabolic imaging of liver metastasis at 7 T. NMR Biomed 2020;33(4):e4221.
47. Kitamura K, Shirato H, Seppenwoolde Y, et al. Tumor location, cirrhosis, and surgical history contribute to tumor movement in the liver, as measured during stereotactic irradiation using a real-time tumor-tracking radiotherapy system. Int J Radiat Oncol Biol Phys 2003;56(1): 221-228.
48. Shirato H, Seppenwoolde Y, Kitamura K, Onimura R, Shimizu S. Intrafractional tumor motion: Lung and liver. Semin Radiat Oncol 2004; 14(1):10-18.

49. van Houtum Q, Welting D, Gosselink WJM, et al. Low SAR ^{31} P (multi-echo) spectroscopic imaging using an integrated whole-body transmit coil at 7T. NMR Biomed 2019;32(12):e4178.

50. van Houtum QQ, Mohamed Hoesein FFAA, Verhoeff JJJC, et al. Feasibility of ^{31} P spectroscopic imaging at 7 T in lung carcinoma patients. NMR Biomed 2021;34(5):e4204.

51. Van den Wildenberg L, Gursan A, Seelen LWF, et al. Test-retest reliability of in-vivo 31P MRSI of the whole human liver at 7 tesla using a 31P whole-body transmit coil and 16-channel receive array. *Proceedings of the 2022 Joint Annual Meeting ISMRM-ESMRMB & ISMRT 31st Annual Meeting*. p 2291.